

Enhancing the Electrical Properties of Porous Silicon Photodetector by Depositing MWCNTs

Ahmed N. Abd^{1*}, Nadir F. Habubi², Ali H. Reshak³ and Hazim L. Mansour¹

¹Physics Department, Education Faculty, University of Mustansiriyah, Baghdad, Iraq.

²Physics Department, Science Faculty, University of Mustansiriyah, Baghdad, Iraq.

³New Technologies - Research Centre, University of West Bohemia, Univerzitni 8, 306 14 Pilsen, Czech Republic.

³Center of Excellence Geopolymer and Green Technology, School of Material Engineering, Universiti Malaysia Perlis, 01007 Kangar, Perlis, Malaysia.

Received 18 June 2017; Revised 8 December 2017; Accepted 17 January 2018

ABSTRACT

In the present work, multiwall carbon nanotubes (MWCNTs) layers dispersed in DMF and citric acid deposited by drop casting on porous silicon (PSi) photodetector have been prepared by electrochemical etching (ECE) process at 25 mA/cm² for 20 min. X-ray diffraction (XRD), atomic force microscopy (AFM), Fourier transformation infrared spectroscopy (FTIR), energy dispersive X-ray (EDX), current-voltage (I-V) characteristics, capacitance-voltage (C-V) characteristics, spectral responsivity (R_s) and specific detectivity (D) before and after depositing MWCNTs layers were investigated. It was found that, the On/Off ratio was increased after depositing MWCNTs, while ideality factor and built in potential were decreased and this fact indicates that Al/PSi/c-Si/Al photodetector was nearly approaching the ideal diode characteristic after deposition process. Significant enhancement in spectral responsivity and specific detectivity were also noticed after depositing MWCNTs on porous matrix.*

Keywords: MWCNTs; PSi; ECE; Electrical Properties; Photodetector.

1. INTRODUCTION

It is well known that, the discovery of carbon nanotubes CNTs in 1991 by Iijima [1] has revolutionized the research in the carbon field, in spite of the fact that the first manufacturing of the CNTs was in 1960 by Bacon [2]. Iijima had realized that CNTs can be obtained by rolling a sheet of graphene onto itself, and multiwall carbon nanotubes (MWCNTs) can be obtained by several concentric single-walled CNTs [1].

MWCNTs have many features, such as, thermal and chemical stability, very light weight, large tensile strength and good electronic properties, which made MWCNTs materials offer tremendous potential applications in science and technology [3-6]. The inner CNTs are usually protected from any outside chemical interactions by outer walls on the MWCNTs. The tensile strength of the MWCNTs is known to be higher than SWCNTs [7]. Electrical properties exhibited by MWCNTs might be different from their SWCNTs counterparts, for example, the SWNTs band gap can be changed from zero to 2.0 eV. Therefore, a semiconducting and metallic behavior can be revealed [8, 9]. Thus, the above mentioned properties might made CNTs as a good candidate for tremendous applications, such as conductive materials [10, 11], microwave and electromagnetic absorbing coating, composites of high strength [12], fibers [13, 14], sensors

*Corresponding Author: nadirfadhil@uomustansiriyah.edu.iq

[15], field emission displays [16], devices for the conversion and storage of energy [17] and semiconductor devices of nanometer-sized and radiation sources [18]. A great interest has been stimulated for the use of CNT for photovoltaic field, due to its ability of tuning the band gap for a large range making use of the adjustment of diameter of the carbon tube with excellent optical and electronic properties [19]. In future, for the optoelectronic devices, the CNTs might be considered as Si best replacement [20, 21]. The present research aims to use MWCNTs for the fabrication porous silicon photodetector.

2. EXPERIMENTAL PROCEDURE

A mirror-like monocrystalline silicon wafer having resistivity of $10 \Omega \cdot \text{cm}$ and an orientation of (100) was employed for the fabrication of a photodetector p-type porous silicon (p-PSi) by electrochemical etching (ECE) process, the ECE process was conducted by employing a cell of Teflon full of electrolyte which contains hydrofluoric acid with 48% concentration and also an ethanol with purity 99.9%, 1:2 volume. The Si wafer was treated chemically and thick Al layer was deposited on the back face using thermal evaporation process. The p-PSi samples were etched at 25 mA/cm^2 for 20 min. MWCNTs powder was obtained from Nano. Tech. Lab. The diameter was about (20-75) nm and length was about (8-20) μm . MWCNTs was dispersed in DMF and citric acid and sonication to 12h to debundle MWCNTs. Drop casting technique was employed to deposit p-PSi with MWCNTs by taking the solution by pipette and then dropped on PSi substrate. Figure (1) exhibits cross-sectional view of MWCNTs layer, which was deposited on porous matrix.

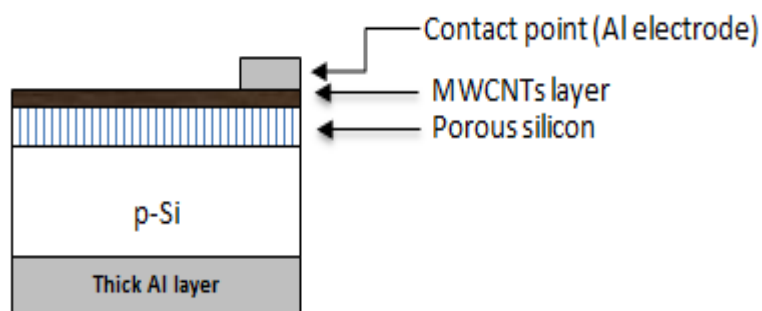


Figure 1. Diagram of photodetector showing MWCNTs layer deposited on porous silicon.

Different physical properties of porous silicon and MWCNTs-deposited PSi were studied by using (XRD-6000, Shimadzu X-ray diffractometer, Japan), Fourier transformation infrared spectroscopy, transmission electron microscopy type Philips CM10 pw 6020 and AFM (Atomic Force Microscope) type Angstrom AA 3000. The deposited and *un*-deposited photodetectors spectral photosensitivity measurements in the wavelength range 400-950 nm were carried out by employing a (Joban-Yvon monochromator), which was calibrated by using a Sanwa silicon power meter. All the measurements were performed at room temperature.

3. RESULTS AND DISCUSSION

X-ray diffraction for p-Si is shown in Figure (2-a) from which it can be observed a sharp peak located at 33.5° diffraction angle with (211) reflecting plane of cubic structure of p-Si (according to 1997 JCPDS 17-0901), which was approved the single crystal structure of c-Si. Figure (2-b) shows the X-ray diffraction of p-PSi sample etched at 25 mA/cm^2 anodization current density for 20 min anodization time. A splitting and broadening peak were observed around the 33.35°

diffraction angle, which had the same direction. This might be attributed to the decrease in crystallinity of Si wafer after etching toward nanocrystal size. However the etched silicon still had the single crystal structure even after etching process.

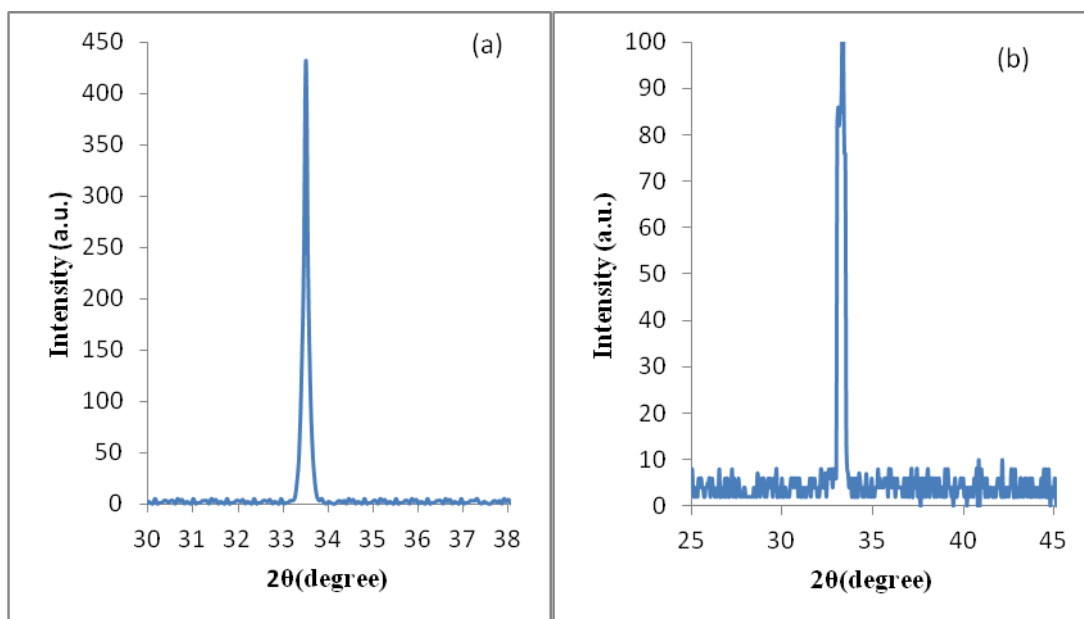


Figure 2. XRD spectra of (a) p-Si, (b) p-PSi sample at etching time of 20 min and an anodization current density of 25mA/cm².

Figure (3) exhibits 3D AFM image and the chart of the granularity cumulation distribution for the etched p-Si, the average pore diameter, root mean square, roughness average and ten point height, which were found to have values of about 36.15 nm, 1.52 nm, 1.29 nm and 6.2 nm, respectively. From the 3D AFM image the pore type was found to be mesoporous.

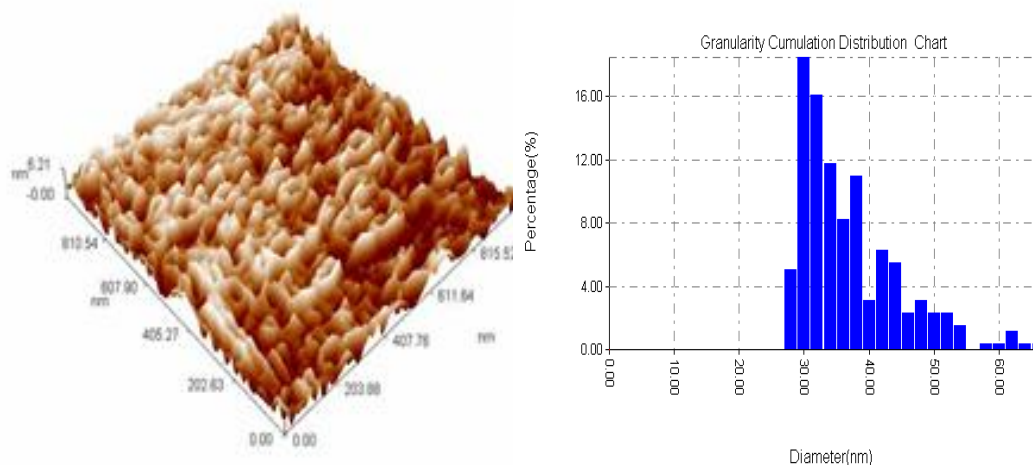


Figure 3. 3D AFM image and granularity cumulation distribution chart of p-PSi prepared at 20min etching time and 25 mA/cm² etching current density.

The FTIR spectra of the PSi substrate are shown in Figure (4). A strong broad band was observed at about 1080.17 cm⁻¹ due to Si-O-Si asymmetry stretching vibrations mode in PSi, which was dependent on the oxidation degree of porous silicon. The other IR bonds were listed in Table (1).

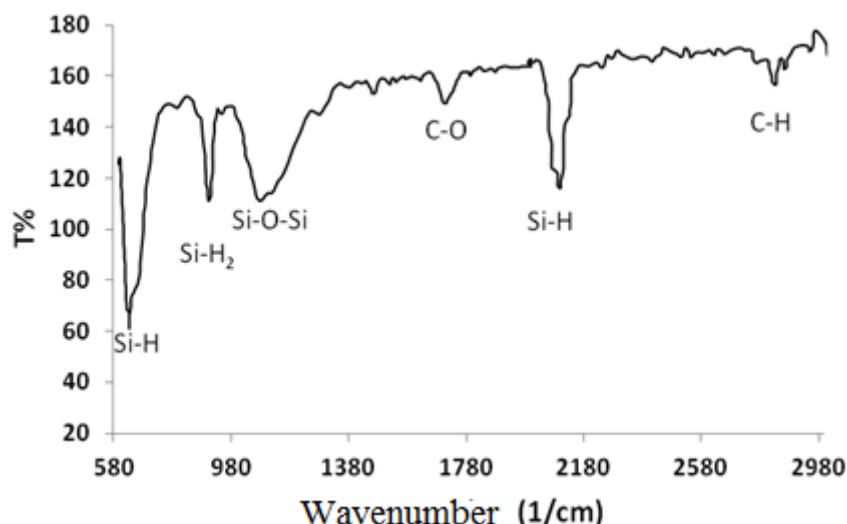


Figure 4. FTIR spectra of the p-PSi prepared at etching time of 20 min and etching current density of 25mA/cm².

Table 1 Chemical bonds and their IR resonance positions in p-PSi

Functional groups	Frequency(cm) ⁻¹	Bonds	Vibration mode
Si-H	621, 2091	Si ₃ -SiH	Bending modes
Si-H ₂	908.47	Si-H ₂	Scissor modes
Si-O-Si	1080.17	Si-O-Si	Asymmetric stretch
C-H	2939.52	C-H ₂	Asymmetric stretch
C-O	1703.2	C-O	Carbon Oxygen bond

Figure (5-a, b) represents EDX investigation for PSi before and after the deposition of MWCNTs respectively. Oxygen concentration was decreased after the deposition of MWCNTs and this might be attributed to the reduction of oxygen from the pore and the incorporation MWCNTs in that pores. The presence of oxygen, silicon and fluorine were due to the porous silicon structure. In Figure (5-b) The presence of a peak near 3 KeV after the deposition might be due to the cleaning process by argon ion bombardment prior to CNTs deposition, which made Si pores (partially) filled by Ar.

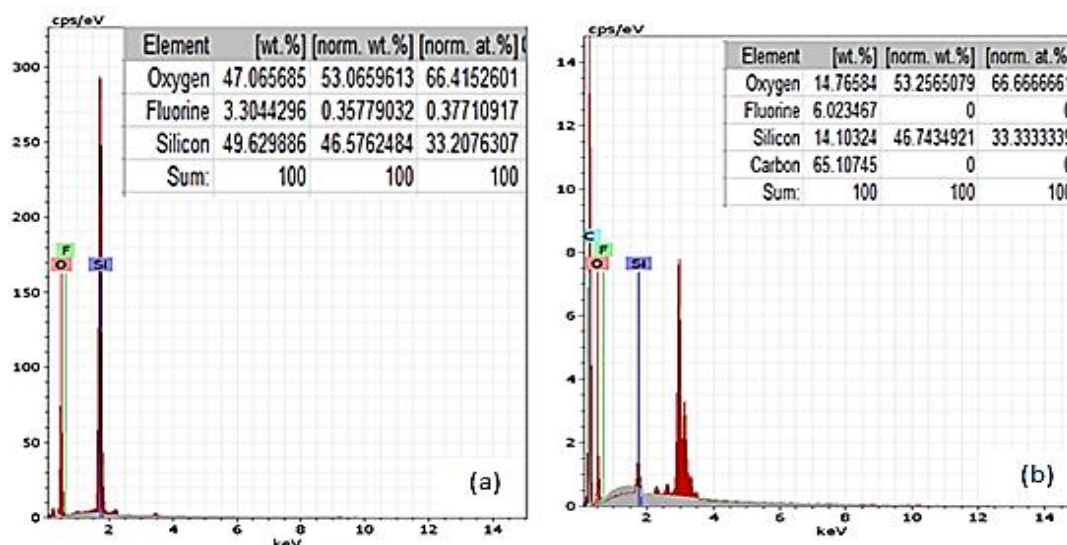


Figure 5. EDX of p-PSi (a) before (b) after the deposition of MWCNTs layers.

Figure (6) shows the illuminated current density under reverse biasing swept from -10 V to +10 V (under power density $6445 \mu\text{W}/\text{cm}^2$) of Al/PSi/p-Si/Al and MWCNTs/PSi/p-Si/Al photodetectors. As can be observed from Figure (6), the illuminated current density of Al/PSi/p-Si/Al photodetector was increased after the deposition of MWCNTs. This was occurred because MWCNTs act as photogeneration, which was able to generate electron-hole pairs upon illumination. The ideality factor was 3.7 for Al/PSi/p-Si/Al and it was decreased to 1.9 after the deposition of MWCNTs, i.e. MWCNTs have enhanced the electrical properties of Al/PSi/p-Si/Al photodetector, made it close to an ideal diode [22]. The On/Off ratio (which represent the ratio of illuminated to dark current) was 1449 for Al/PSi/p-Si/Al and was increased after the deposition of MWCNTs to 2124. This was occurred by the increasing of illuminated current after depositing MWCNTs. This might be due to the semi-metallic property of the MWCNTs, the heterojunction is expected to have better conductivity and therefore reduce the series resistance effect [23].

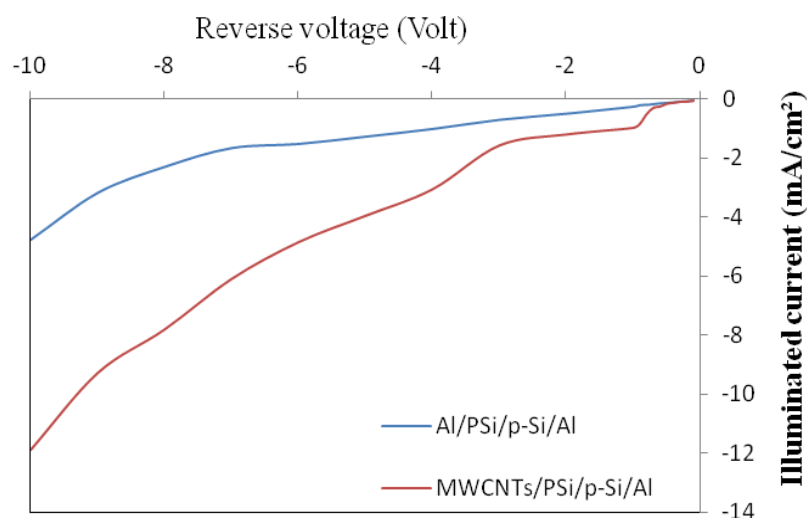


Figure 6. Illuminated I-V characteristics under reverse biasing of both Al/PSi/p-Si/Al and MWCNTs/PSi/p-Si/Al.

Figure (7) exhibits the C-V characteristics under reverse bias voltage ranging from 0-6 V, from which one can observe that the capacitance was decreased with increasing the reverse bias voltage. This might be due to the width increment of depletion region, which causes a capacitance decrement at the junction.

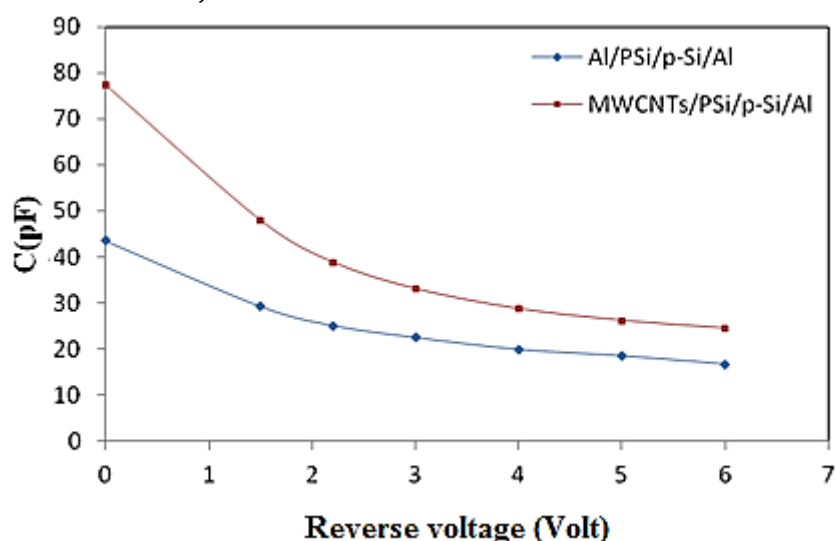


Figure 7. C-V characteristic plot for both Al/PSi/p-Si/Al and MWCNTs/PSi/p-Si/Al photodetectors.

Figure (8), illustrates a linear relationship between C^{-2} versus reverse bias voltage. This figure confirmed that the junction between PSi/p-Si and MWCNTs/PSi is an abrupt junction. The value of built in potential decreased from 1.1 eV to 0.6 eV after the deposition of MWCNTs, i.e. the electron required smaller energy to transfer from MWCNTs to PSi, in case of the deposition of MWCNTs onto PSi layer, and these were expected to depend on the Fermi level position in the conduction band at high carrier concentrations.

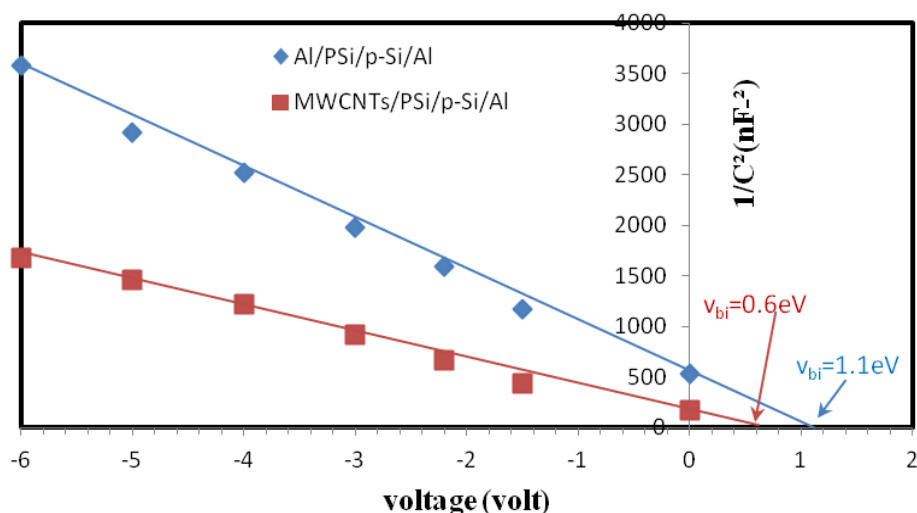


Figure 8. $1/C^2$ against reverse voltage for Al/PSi/p-Si/Al and MWCNTs/PSi/p-Si/Al photodetectors.

Figure (9) shows Al/PSi/p-Si/Al and MWCNTs/PSi/p-Si/Al photodetectors spectral responsivity. The responsivity of Al/PSi/p-Si/Al was increased from 0.61 A/W to 0.87 A/W at 800 nm after depositing MWCNTs layers. This improvement might be ascribed to have increment in the absorption of surface area due to the presence of MWCNTs and also because of increasing the depletion width and diffusion length. The above results might suggest that an important role was played by the silicon substrate in the present device, in addition to a photocurrent, which was generated due to MWCNTs. The obtained results have shown a good agreement with the results reported by Ismail *et al.* [22].

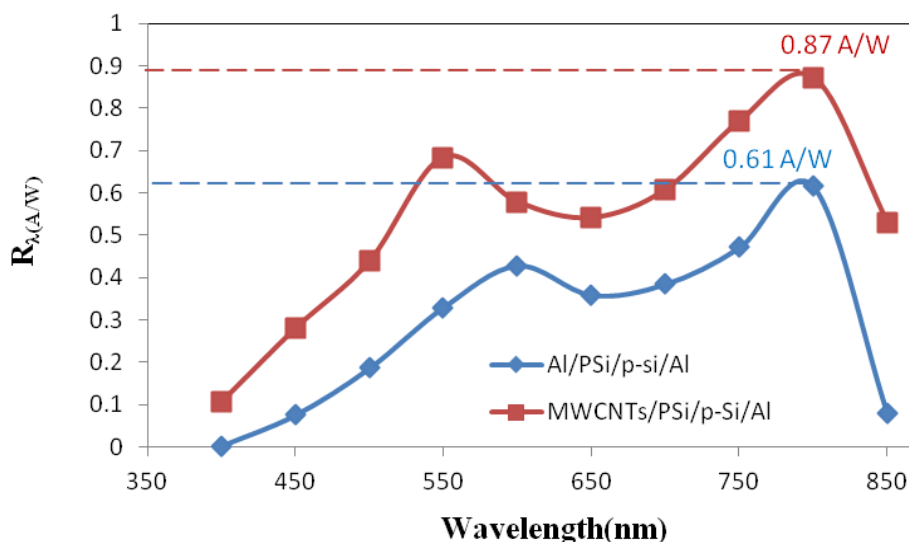


Figure 9. Spectral responsivity versus wavelength of Al/PSi/p-Si/Al and MWCNTs/PSi/p-Si/Al photodetectors.

As can be seen from Figure (10), the specific detectivity of Al/PSi/p-Si/Al photodetector has a maximum value of about $5.6 \times 10^{13} \text{ W}^{-1} \cdot \text{cm} \cdot \text{Hz}^{1/2}$ at 800 nm. This value was increased after

depositing MWCNTs to about $7.88 \times 10^{13} \text{ W}^{-1} \cdot \text{cm} \cdot \text{Hz}^{1/2}$ at 800 nm and this might be attributed to Van Hove singularities, which were responsible for the e-h pair generation and related to the electronic transition in the density of state of each single wall carbon nanotube [24]. Thus, MWCNTs acted as building blocks for photodetectors. The improvement of specific detectivity might be attributed to the decreasing of both concentrations of structural defects and noise current and the increasing in spectral responsivity.

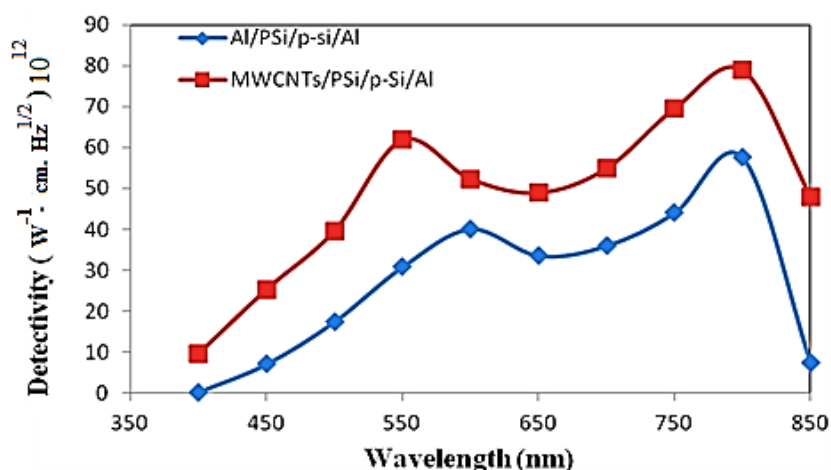


Figure 10. Specific detectivity plots for Al/PSi/p-Si/Al and MWCNTs/PSi/p-Si/Al photodetectors.

4. CONCLUSIONS

A simple and efficient approach to improve the photoresponse and photovoltaic properties of silicon matrix photodetectors prepared by anodization technique via depositing with suspension MWCNTs dispersed in DMF is presented. The enhancement in photo-response and photovoltaic properties were explained via the increasing of the absorption coefficient and carrier diffusion length as well as by the carrier transfer from MWCNTs to porous silicon. The results have shown that mono-crystalline porous structure of random distributed nanocrystallite pillar silicon having same direction. I-V characteristics indicated an improved charge transfer between porous and electrode and an increased photocurrent after MWCNTs layer depositing. The decrease in ideality factor from 3.7 to 1.9 enhanced photosensitivity to 0.87 A/W and the high specific detectivity to $7.88 \times 10^{13} \text{ W}^{-1} \cdot \text{cm} \cdot \text{Hz}^{1/2}$ at 800 nm and also increased On/Off ratio to a significant enhancement of the porous heterojunction performance after the MWCNTs layer deposited. The high photosensitivity at visible and near-IR regions approved that this method is suitable to be used in the fabrication of silicon photodetectors for the detection of weak optical signals. Thus the obtained high photodetectors performance has validated the method employed in the present study.

ACKNOWLEDGEMENTS

The authors would like to thank Al-Mustansiriya University (www.uomustansiriya.edu.iq) Baghdad -Iraq for their support in the present work.

REFERENCES

- [1] S. Iijima: *Nature* **354** (1991) 56.
- [2] R. Bacon: *J. Appl. Phys.* **31** (1960) 283.
- [3] C. Klumpp, K. Kostarelos, M. Prato, A. Bianco, *Biochem. Biophys. Acta* **1758** (2006) 404.
- [4] Z. Liyun, L. Hongyun, H. Naifei. *J Colloid. Interface Sci.* **296** (2006) 204
- [5] Qingxin Mu, Wei Liu, Yuehan Xing, Hongyu Zhou, Zhenwei Li, Ying Zhang, Leihua Ji, Fang Wang, Zhikun Si, Bin Zhang, and Bing Yan. *Phys. Chem. C* **112** (2008) 3300.
- [6] J. Kathi and K. Y. Rhee. *J Mater. Sci.* **43** (2008) 33.
- [7] Carbon nanotube. In Wikipedia, The Free Encyclopedia (2008, April 24). Retrieved 03:04, April 28.
- [8] P.J.F. Harris, *Carbon Nanotubes and Related Structures: New Materials for the Twenty-First Century*, Cambridge University Press, New York, (1999).
- [9] L. Dai (Ed.), *Carbon Nanotechnology: Recent Developments in Chemistry, Physics, Materials Science and Device Applications*, Elsevier, Amsterdam, (2006).
- [10] Z.J. Fan, T. Wei, G.H. Luo, F. Wei, *J. Mater. Sci.* **40** (2005) 5075
- [11] K. Kordas, T. Mustonen, G. Toth, H. Jantunen, M. Lajunen, C. Soldano, S. Talapatra, S. Kar, R. Vajtai, P.M. Ajayan, *Small* **2** (2006) 1021.
- [12] J.N. Coleman, U. Khan, Y.K. Gun'ko, *Adv. Mater.* **18** (2006) 689
- [13] K.L. Jiang, Q.Q. Li, S.S. Fan, *Nature* **419** (2002) 801
- [14] M. Zhang, K.R. Atkinson, R.H. Baughman, *Science* **306** (2004) 1358
- [15] J.H. Liu, J.Y. Liu, L.B. Yang, X. Chen, M.Y. Zhang, F.L. Meng, T. Luo, M.Q. Li, *Sensors* **9** (2009) 7343.
- [16] S.S. Fan, M.G. Chapline, N.R. Franklin, T.W. Tomblor, A.M. Cassell, H.J. Dai, *Science* **283** (1999) 512.
- [17] H. Zhang, G.P. Cao, Y.S. Yang, *Energy Environ. Sci.* **2** (2009) 932.
- [18] Q. Cao, J.A. Rogers, *Adv. Mater.* **21** (2009) 29
- [19] R. Saito, G. Dresselhaus, and, M. S. Dresselhaus, "Physical Properties of Carbon Nanotubes," *Imp. Coll. London*, (1998).
- [20] E. S. Snow, P. M. Campbell, M. G. Ancona, and J. P. Novak, *Appl. Phys. Lett.*, **86** (2005)1.
- [21] J. Appenzeller, *Proc. IEEE*, **96** (2008) 201.
- [22] Raid A. Ismail, Raheem G. Kadhim, Wasna'a M. Abdulridha, *Optic* **127** (2016) 8144.
- [23] Dali Shao, Mingpeng Yu, Jie Lian, Shayla Sawyer, *Appl. Phys. Lett.* **102** (2013) 021107-3.
- [24] Paola Castrucci, Claudia Scilletta, Silvano Del Gobbo, Manuela Scarselli, Luca Camilli, Mirko Simeoni, Bernard Delley, Alessandra Continenza and Maurizio De Crescenzi *Nanotechnology* **22** (2011) 115701.